

MOLECULAR DOCKING OF FLUORINATED HETEROCYCLIC SULFONAMIDES: NOVEL LIGANDS WITH SELECTIVE AFFINITIES FOR HUMAN AND *PLASMODIUM* DIHYDROFOLATE REDUCTASE

Akesh Mallia**, Miki Nguyen*^{+,++}, Joseph Sloop, and Neville Forlemu[†]

School of Science & Technology (Chemistry), Georgia Gwinnett College, Lawrenceville, GA 30043

^{**}School Without Walls High School, 2130 G St. NW Washington, DC 20037⁺⁺The Gwinnett School of Mathematics, Science, and Technology, Lawrenceville, GA 30044

Abstract

Parasitic resistance and mutations in folate pathway receptors of *Plasmodium falciparum* have diminished the efficacy of antimalarial agents including sulfadoxine and pyrimethamine. In this study, seven novel fluorinated heterocyclic sulfonamides are modeled to determine their potential to blunt the effects of folate pathway mutations such as those on dihydrofolate reductase (DHFR). With AutoDock Vina and the Molecular Operating Environment (MOE), binding affinities and interactions of the fluorinated sulfonamides are benchmarked with antimalarial drugs. The binding affinity scores from both programs identify three sulfonamides with strong interactions that are comparable to or greater than current antimalarials. Compound 7 displayed strong hydrogen bonding interactions with quadruple mutated *P. falciparum* DHFR active site residues and an estimated binding energy of -7.6 ± 0.2 kcal/mol. From further interaction analysis, the fluorinated heterocyclic sulfonamides modeled herein seem to be promising pharmacophores and competitors to current folate pathway inhibitors.

[†]Corresponding author: nforlemu@ggc.edu^{***} High school and undergraduate researchers and co-authorsKeywords: Fluorinated sulfonamides, docking, AutoDock Vina, MOE, Dihydrofolate Reductase, *Plasmodium falciparum*, binding energy

Received: January 27, 2023

Accepted: February 17, 2023

Published: March 16, 2023

Introduction

Malaria is a deadly disease that adversely affects the health and economies of numerous communities worldwide, and whose effects have worsened following the COVID-19 pandemic.¹ *Plasmodium falciparum*, the most virulent malarial parasite, relies on the folate pathway for the biosynthesis of metabolites.² In particular, dihydrofolate reductase (DHFR) is a key folate pathway enzyme that has been targeted by multiple antifolate and antimalarial drug agents like pyrimethamine and sulfadoxine.³⁻⁵

Antifolate drug resistance is associated with the rise of mutations in DHFR enzyme isoforms, with three mutations prevalent in the African region: N51I, C59R, and S108N.⁵ An additional mutation, I164L, mostly reported in Asia and South America, provides high levels of resistance against antimalarials like pyrimethamine.⁶ Steric clashes resulting from A16V, and S108T are responsible for cycloguanil resistance.⁷ According to Sirawaraporn and collaborators, there is a 300 to 600-fold increase in inhibition constant (K_i) in interactions with antimalarial ligands (pyrimethamine and cycloguanil) with the DHFR quadruple mutant compared to the wild type enzyme.³

This study explores two main questions: 1. Do ligands with fluorinated sulfonamide frameworks interact with folate enzymes (DHFR) with affinities comparable to benchmark antifolate and antimalarial drugs? 2. Do the rampant mutation in *Plasmodium* folate pathway enzymes (DHFR variants) impact the affinities of fluorinated sulfonamides?

Molecular Structures and Properties

The binding of DHFR isoforms with current antimalarial drugs and sulfonamide derivatives developed in this laboratory and with

collaborators was modeled as described below (Compounds 1-7 in Figure 1B). The sulfonamide framework was fine-tuned with the inclusion of fluorine atoms and heteroaromatic amines to modulate polar surface area, rigidity, and drug-like properties. The sulfonamides were built with GaussView, and optimized with Gaussian 09 using the B3LYP/6-311g basis set.^{8,9} The three dimensional structures of antifolate and antimalarial drugs were obtained from the DrugBank database and are represented in Figure 2.¹⁰

The three-dimensional structures of human DHFR (Wt HsDHFR and pdb-ID-3GYF)¹¹, and wild type (Wt PfDHFR and pdb-ID-

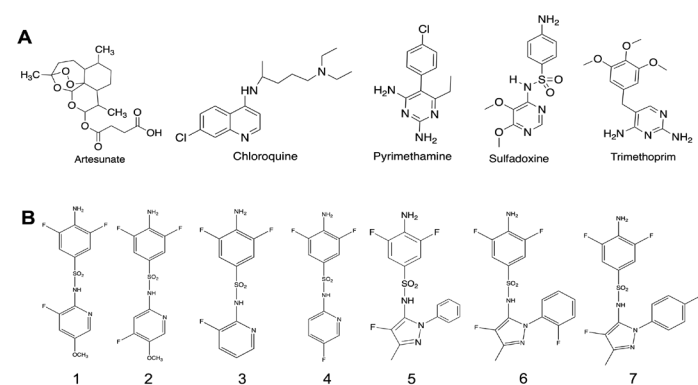


Figure 1: A Antifolate and antimalarial drugs used. B Heterocyclic sulfonamide derivatives. 1 (2-(4-amino-3,5-difluorophenylsulfonamido)-3-fluoro-5-methoxypyridine) 2 (2-(4-amino-3,5-difluorophenylsulfonamido)-4-fluoro-5-methoxypyridine) 3 (2-(4-amino-3,5-difluorophenylsulfonamido)-3-fluoropyridine) 4 (2-(4-amino-3,5-difluorophenylsulfonamido)-5-fluoropyridine) 5 5-(4-amino-3,5-difluorophenylsulfonamido)-4-fluoro-3-methyl-1-phenylpyrazole 6 5-(4-amino-3,5-difluorophenylsulfonamido)-4-fluoro-3-methyl-1-(2-fluorophenyl)pyrazole 7 5-(4-amino-3,5-difluorophenylsulfonamido)-4-fluoro-3-methyl-1-(4-fluorophenyl)pyrazole

4DPD)¹² double mutant (DM PfDHFR and pdb-ID-3UM6)⁷ and quadruple mutant (QM PfDHFR and pdb-ID-4DP3)¹² Plasmodium DHFR were downloaded from the RCSB Protein Data Bank.¹³

The similarity of the ligands to drugs was modeled using the SwissADME webtool and displayed in Figure 2.¹⁴ Through SwissADME, drug-like molecules are identified by comparing molecules to a database of known drugs, functional groups, and properties that are favorable for drug design. The resulting pharmacokinetic properties were compared with antimalarial drugs in this study.

Molecular Docking Methods

In this study, the interactions between the 12 ligands (7 heteroaromatic sulfonamides and 5 antimalarial drugs) and *P. falciparum* DHFR variants (Wt HsDHFR, Wt PfDHFR, DM PfDHFR, QM PfDHFR) were modeled using two major docking tools: AutoDock Vina and the Molecular Operating Environment (MOE).¹⁵⁻¹⁷ The USCF Chimera tool Dock Prep was used to refine the receptor molecules by removing solvents, fixing non-standard residues, adding hydrogens, and assigning Gasteiger charges.¹⁵⁻¹⁷ AutoDock Vina software was then employed to perform a global search of the best bound complexes, which were then ranked and scored based on favorable hydrophobic, hydrogen bond, and van der Waals interactions. This was performed using the protein and ligand coordinates along with a search volume box with size 25 Å x 22 Å x 32 Å centered around the binding sites of DHFR. The proteins and ligands were rigid during the docking, and the complexes with root-mean square deviations (RMSD) less than 1.0 Å were clustered according to their energy of binding. The docked complexes with the lowest binding energies were then extracted for further analysis.

The Molecular Operating Environment (MOE) software was also used to characterize the interaction affinity between the ligands and DHFR receptors. Each optimized ligand was uploaded into an MOE window, subjected to 3D protonation and energy minimization, and saved in a molecular database (MDB) file for docking. The crystal structures for each receptor were uploaded into MOE, and prepared for docking using the QuickPrep feature of MOE as described by Al-Karmalawy and Khattab.^{15,18,19} This involved the addition of hydrogens in appropriate geometries, removal of solvent molecules, and minimization of the structure to relax atomic clashes and correct protein issues. The docking simulation was done using the 2 MOE default forcefields (CHARMM27 and Amber10: EHT), with atoms tethered 8 Å around the active site, allowing for enhanced flexibility of site molecules during the docking process. The docking site was selected as receptor atoms, the ligand placement methodology with triangle matcher, and the London dG scoring function to estimate the free energy of binding. The refinement methodology was adjusted as Induced Fit, with a scoring function based on GBVI/WSA dG to select the 5 best poses out of 30 for each ligand/receptor system.

Results

Drug-like Properties of Fluorinated Sulfonamides

Compounds with good drug-like features often have a topological polar surface area (TPSA) of less than 120 Å², enabling high absorption.²⁰ The TPSA of **1** and **7** are within this upper bound

and are within 25 Å² of the TPSA of artesunate. The TPSA of chloroquine was much lower than the other ligands tested. When comparing to experimental results, the TPSA from SwissADME correlated with a previous study on chloroquine within 1 Å².²¹ The solubility of a drug in the mostly aqueous environment of nearly all biological systems is another important property computed for the novel sulfonamides.²² Compounds **1-4** are labeled soluble while **5-7** are labeled moderately soluble. The sulfonamides represented in this study also possess ADME properties that make them suitable drug candidates and comparable to current antimalarial drugs (Figure 2).²³

Binding Energy of Fluorinated Ligands

To estimate the affinity and viability of sulfonamides as potential antimalarial agents, 48 docking simulations between 12 ligands and the 4 target receptors were performed using AutoDock Vina and MOE. The docked complexes of five current antimalarial drugs were compared to fluorinated heteroaromatic sulfonamides. For each docked system, 8 high affinity complexes were analyzed for key binding domains and contact residues responsible for interactions. The impact of mutations on binding was also sought in the docking simulations. Since the location of all six mutations explored (A16V, S108T, N51I, C59R, S108N, I164L) were proximal to the active site, another round of docking was conducted, focusing on the active site using MOE. The binding affinities of the fluorinated sulfonamide ligands and target receptors are represented in Figure 3A, B, and C.

The fluorinated heteroaromatic sulfonamides (**5**, **6**, and **7**) show stronger affinity with the DHFR enzymes compared to some antimalarial drugs (notably pyrimethamine and trimethoprim). Although the benchmark medication for treating malaria has been artesunate over the last couple of decades, blind docking relative binding energies from MOE and AutoDock Vina indicate a decrease in interaction affinity with mutated DHFR receptors (Figure 3A and B). Similarly, the blind docking with AutoDock Vina identifies an alternate binding site that is more favorable to bind-

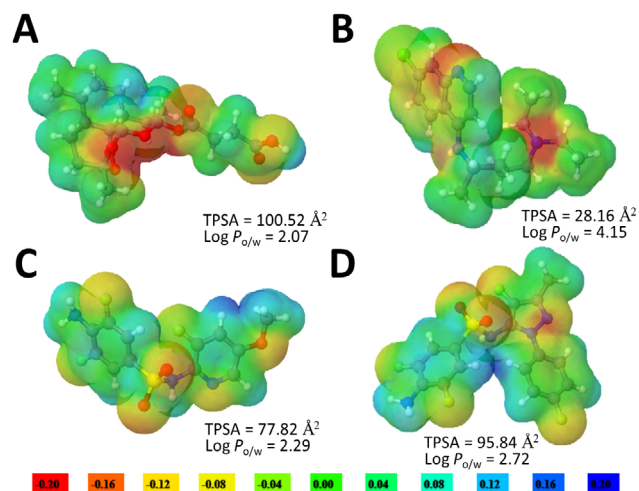


Figure 2: Electrostatic potential map of the following ligands: **A.** Artesunate, **B.** Chloroquine, **C.** Compound **1**, **D.** Compound **7**. Partial negative charges shown in red and partial positive charges shown in blue. Topological Polar Surface Area (TPSA) is described in Angstroms squared. Lipophilicity (Log P_{o/w}) is based on consensus between five methods of prediction.

ing artesunate than the active site region. The mutations from wild type DHFR to double mutant and quadruple mutant DHFR also diminish the affinity of chloroquine, pyrimethamine, and trimethoprim (Figure 3A and B).

In all the blind docking simulations using AutoDock Vina and MOE, the DHFR active site was the preferred binding domain for 1-7, pyrimethamine, and sulfadoxine. In docking simulations where the search area is constrained to the active site of DHFR, more favorable contacts between artesunate, chloroquine and DHFR mutant enzymes are observed as well (Figure 3C). An interesting observation with sulfonamides is that ligand rigidification with the addition of the heteroaromatic ring to the fluorinated sulfonamide pharmacophore (5-7) enhances the binding affinity to match artesunate. In addition, irrespective of the docking methodology and software used, the strength of the interactions between heterocyclic sulfonamides also does not diminish in the presence of the mutations in the double and quadruple mutant DHFR receptors (Figure 3). The rigidification and enhancement of the lipophilicity of the sulfonamides have a stabilizing effect on the complexes formed (Figure 3). The docking data from AutoDock Vina (Figure 3A) and MOE (Figure 3B) share similar trends. For example, the docked complexes with 1-4 are not as stable or favorable as those involving 5-7. In addition, the blind docking data

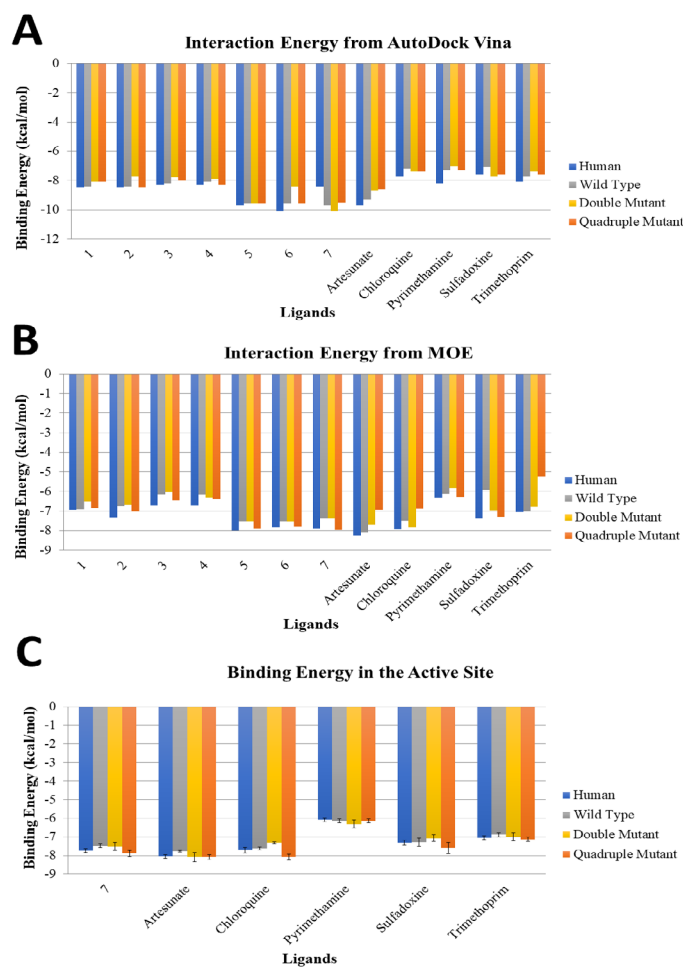


Figure 3. A. AutoDock Vina relative binding energies between benchmark drugs, fluorinated sulfonamides, and DHFR isoforms. B. MOE relative binding energies using the site location found by AutoDock Vina. C. MOE relative binding energies focused on the active site with error bars indicating standard deviation over docking poses.

suggest that the mutations have an impact on the binding affinity of artesunate (Figure 3A and 3B) while 5-7 complexes bind QM PfDHFR with comparable or stronger affinity to Wt PfDHFR. One important difference is the favorability of chloroquine complexes which rival that of artesunate using MOE compared to AutoDock Vina.

Binding Domains and Residues with Fluorinated Sulfonamides

The antifolate and antimalarial agents modeled in this study dock with DHFR receptor isoforms mainly using two binding domains (Figure 4). These include the active site and its surrounding domains which was the most favorable pocket for DHFR, and an allosteric site identified by blind docking using AutoDock Vina (Figure 4D). All docking poses analyzed for the interactions between the fluorinated heteroaromatic sulfonamides (e.g., 7) occur in regions close to or at the active site of DHFR (Figure 5). This is not the case with the benchmark antimalarial drug artesunate, where AutoDock Vina places artesunate in an alternate site when docked to quadruple mutant DHFR (Figure 4D). This alternate binding domain has a lower binding energy (Figure 3B) compared to docking poses with artesunate constrained in the active site (Figure 3C). In this section we compare the most favorable binding poses involving artesunate and 7 with DHFR (Figure 4 and 5). The combinations of hydrophobic domains (green), polar domains (pink) and the exposed areas of the receptor (red) were responsible for strong interactions. The labeled and highlighted residues contributed strongly (greater than -0.5 kcal/mol) to stabilization of artesunate and 7 in the binding site (Figure 4 and 5).

In blind docking where the entire surface of the receptor was sampled for significant interactions, an alternate site was identified for interactions with artesunate using AutoDock Vina. This binding domain was, however, not observed in blind docking with MOE and the ligands. In addition, docked poses where ligands (e.g., 7) were constrained to this alternate binding site used by artesunate with QM PfDHFR (Figure 4D) were not as stable. For example, the alternate site binding energies of -7.6 kcal/mol and

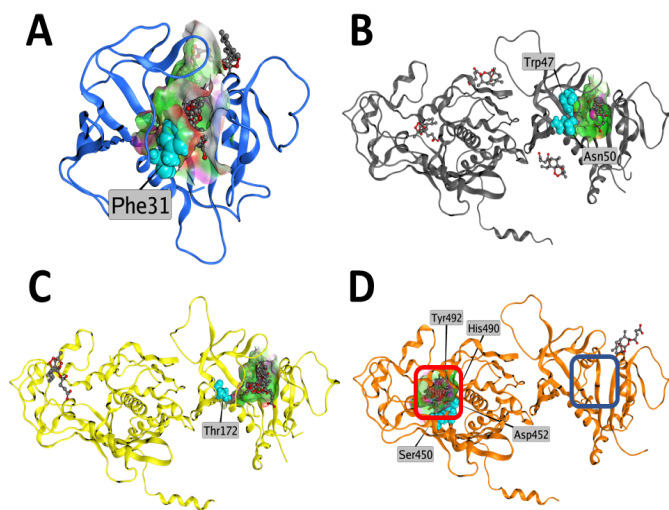


Figure 4. Docking poses of artesunate ligand with DHFR isoforms highlighting important contact residues and different binding domains in the molecule. A. Artesunate with Wt HsDHFR, B. Artesunate with Wt PfDHFR, C. Artesunate with DM PfDHFR, D. Artesunate with QM PfDHFR where the alternate site is shown in the red box and the active site is shown in the blue box

-8.4 kcal/mol were observed between **7** with Wt PfDHFR and DM PfDHFR respectively (computed through AutoDock Vina). These docking scores were both significantly lower than the active site binding energies of -9.7 kcal/mol and -10.1 kcal/mol respectively. Furthermore, to compare the alternate and active sites of DHFR, 2D ligand interaction diagrams were used (Figures 8A and 8B) that display the energetic contribution of different intermolecular contacts that were determined using MOE. Figure 6A depicts artesunate in the alternate site of DHFR (also seen in Figure 4D), whereas Figure 6B depicts artesunate in the active site of DHFR. Both complexes were stabilized by intermolecular forces including hydrogen bonding with the polar oxygens of artesunate. These hydrogen bonding interactions seem to contribute to the majority of artesunate's stable docking scores and its effective pharmacophore structure as an antimalarial drug. The strongest interaction in the alternate site was an ionic contact between His490 and an artesunate oxygen atom contributing about -3.2 kcal/mol to the complex energy.

In the active site complex, the hydrogen bonding interaction where the artesunate carboxylate oxygen atom serves as a hydrogen bond acceptor to Trp48 contributed about -4.5 kcal/mol to the complex energy. This strong association, in combination with hydrophobic and arene-H interaction (-0.8 kcal/mol), explained why the constrained docking with MOE identifies the active site of artesunate as its preferred docking mode. Sulfadoxine is currently used in antimalarial combinations targeted toward children and pregnant women because of its limited side effects. The sulfonamides modeled have a similar pharmacophore structure with Sulfadoxine and both are attracted to the active site of DHFR. The sulfadoxine/QM PfDHFR complex (Figure 6C), is mostly stabilized by intermolecular contacts with an interaction energy smaller than -0.5 kcal/mol. These interactions are weak and generally 3.89 Å distances between contact pairs. The majority of the contacts were arene-H interactions with the amino benzene, with no strong interactions with the sulfonamide functional group. The weaker

interactions explain why the binding energy of sulfadoxine suffers when docked to QM PfDHFR.

In the **7**/QM PfDHFR complex, there were more contacts with energy contributions over -0.5 kcal/mol, and the interactions that occurred were also stronger (Figure 6D) with sulfadoxine. For example, there are three intermolecular contacts (hydrogen bonding interactions) with energy contributions that are greater than -0.5 kcal/mol between **7** and QM PfDHFR (Figure 6D). Compared to sulfadoxine, there were two interactions where amine groups in **7** acted as donors and receptor residues were acceptors. These amine groups provide areas of partial positive charge (Figure 2D and Figure 6D). Similarly, Asn98 served as an H-bond donor to the electronegative oxygen atom part of the **7** sulfonamide group. This shows that the sulfonamide functional group played a critical role in interactions in **7**, whereas for sulfadoxine, it did not contribute positively toward docking. These strong hydrogen bonding interactions may have provided the necessary interaction energy to stabilize the ligand in the active site, overcoming potential repulsive impacts of the mutations on other ligands such as sulfadoxine, pyrimethamine, and trimethoprim.

The complexes of artesunate and **7** in the active site both yielded strong interaction energies (Figure 3C). This result is further supported by the interaction diagrams (Figure 6B for artesunate and Figure 6D for **7**). Both have a particularly strong hydrogen interaction, -4.5 kcal/mol for artesunate and -3.6 kcal/mol for **7**. It should be noted that in Figure 3C, artesunate has about an -0.25 kcal/mol stronger binding affinity than **7** and this might be explained by the overall greater number of contacts with energy contributions of -0.5 kcal/mol and more.

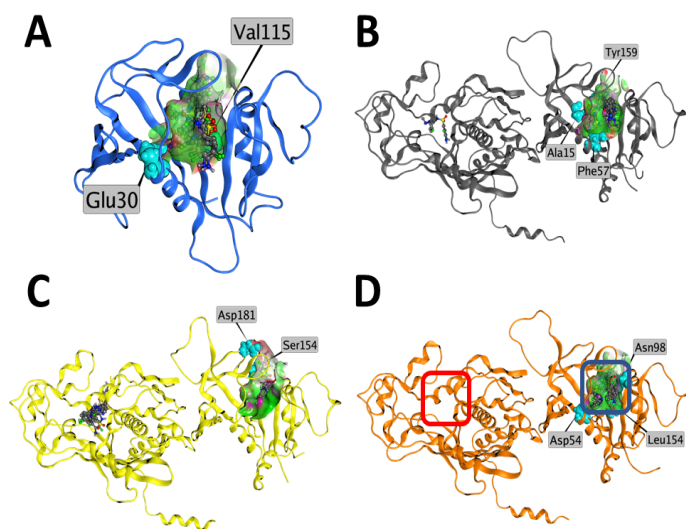


Figure 5. Docking poses of ligand **7** with DHFR isoforms highlighting important contact residues and different binding domains in the molecule. **A.** **7** with Wt HsDHFR, **B.** **7** with Wt PfDHFR, **C.** **7** with DM PfDHFR, **D.** **7** with QM PfDHFR where the alternate site is shown in the red box and the active site is shown in the blue box.

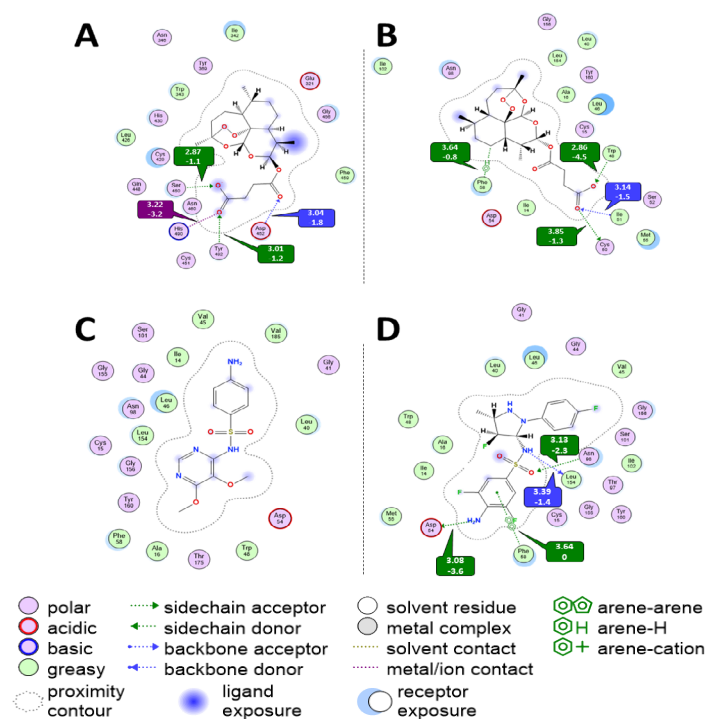


Figure 6. 2D ligand interaction diagram with minimum energy cutoff of -0.5 kcal/mol for hydrogen and ionic interactions. Labels included show the bond distance in Å (top) and the bond energy in kcal/mol (bottom). **A.** Artesunate in the alternate site of QM PfDHFR found by AutoDock Vina. **B.** Artesunate in the active site of QM PfDHFR. **C.** Sulfadoxine in the active site of QM PfDHFR. **D.** **7** in the active site of QM PfDHFR.

Discussion

In this work, the critical residues and docked complexes between the antimalarial and novel fluorinated sulfonamide ligands with DHFR isoforms was modeled and analyzed using AutoDock Vina, Chimera, and MOE. Specifically, the goal was to determine whether the sulfonamide pharmacophore modeled docks to antifolate pathway receptors with affinities similar to benchmark antimalarial drugs. Secondly, the impact of DHFR mutations on the ligands was assessed to determine whether the modeled sulfonamide molecules can maintain high binding affinities in the presence of mutations. Antimalarial or antifolate pathway drugs like artesunate, sulfadoxine and pyrimethamine were used as benchmarks to assess the efficacy of novel sulfonamides as potential antimalarial drugs. Sulfonamides (**5**, **6**, and **7**) containing fluorinated aromatic and heteroaromatic rings are predicted to have binding energies on the same order as the benchmark drugs artesunate and chloroquine. The aforementioned sulfonamides were designed to have similar ADME properties as artesunate (7-8 hydrogen bond acceptor and 3 hydrogen bond donor groups), while utilizing the sulfonamide framework as a pharmacophore (Figure 1 and 2). This translates into multiple interaction sites for binding with DHFR active site residues. The heteroaromatic ring increases their lipophilicity which therefore, provides more opportunities for favorable interactions with amino acid residues in the various receptors (Figure 2). Compounds **1-4** bind to DHFR receptors with a similar energy as the antimalarial drugs sulfadoxine and pyrimethamine. This is an indication that the more polar groups (F and/or N) present in the sulfonamides have a significant impact on the binding process. However, the affinity of **1-4** is smaller compared to artesunate, chloroquine and **5-7**. The addition of the heteroaromatic ring to the sulfonamide ligands plays a significant role in enhancing the affinity of sulfonamide ligands. Amongst all the ligands studied (antimalarial drugs and sulfonamides), the affinity of **5-7** does not seem to diminish in the presence of PfDHFR and the mutant isoforms. This is an indication that the **5-7** pharmacophore framework form strong interactions with DHFR isoforms independent of mutations in amino acid residues observed.

To analyze certain statistical aspects of the results, means and standard deviations of docking scores across the five best poses of the ligands and the active site of DHFR were calculated (Table 1). The overall variability was low and similar between ligand/receptor pairs, ranging between 0.1 to 0.2 kcal/mol. A two-sample equal variance T-Test was also calculated to compare different mean binding energies. Notably, a p-value of 0.1 was found between **7** docked to DM PfDHFR and Wt PfDHFR, meaning that even though binding affinity is slightly decreased with the mutated receptor, this difference is statistically insignificant. Further, while chloroquine docked to QM PfDHFR at a high binding affinity of -7.8 ± 0.2 kcal/mol, the difference in binding energy compared to **7** (-7.6 ± 0.2 kcal/mol) was once again, statistically insignificant (Table 1).

According to Yuthavong et al. (2012), Met55, Phe58 and Arg59 are some of the key residues that make up the active site of DHFR. The MOE Site Finder tool also identifies these as key active site residues and they are present in docking poses where the fluorinated heteroaromatic sulfonamides (such as **7**) are modeled

(Figure 7).⁵ The docking results in this work show the active site of DHFR isoforms as the preferential binding site due to more favorable binding energy ligands such as artesunate and chloroquine (Figure 3C). However, there is an alternate site that accepts multiple ligand poses of artesunate and QM PfDHFR. It is important to determine how the presence of this site compares to the active in QM PfDHFR. The propensity for ligand binding (PLB) of a protein domain can be measured by identifying the compositions of the amino acids involved and comparing that to a profile of the preference that drug-like molecules have toward the 20 standard amino acids.²⁴ In MOE, this method was implemented to determine the PLB of the identified binding sites. Though identified as a viable site in one of the docking methodologies, the alternative site has an estimated PLB value of 0.97. This is about 3 times lower than the estimated PLB value of 2.18 for the active site of DHFR.²⁴ It thus makes sense that when docked to the active site, artesunate was found to have a more favorable binding energy than when docked to the alternate site (Figure 3C). It is notable that the mutations of QM PfDHFR (N51I, C59R, S108N, and I164L) and DM PfDHFR (A16V, and S108T) are proximal to the active site of DHFR (Figure 7). This is a potential reason for why antifolate drugs such as sulfadoxine and pyrimethamine are facing decreased efficacy in that while they may dock in the active site, they are not able to have as many favorable pocket interactions (Figure 6C).

Something especially notable about the binding site of **7** in QM PfDHFR is that it has interactions with two mutated residues, Leu154 and Asn98 (Figure 6D and Figure 7). With Leu154, this is

Table 1: Mean Binding Energies (kcal/mol) of Ligands in the Active Site

Receptor	7	Artemisinin	Chloroquine	Pyrimethamine	Sulfadoxine	Trimethoprim
Hs DHFR	-7.6 ± 0.1	-7.9 ± 0.1	-7.6 ± 0.2	-6.0 ± 0.1	-7.2 ± 0.1	-6.9 ± 0.1
Wt PfDHFR	-7.4 ± 0.1	-7.7 ± 0.04	-7.5 ± 0.1	-6.0 ± 0.1	-7.0 ± 0.2	-6.7 ± 0.1
DM PfDHFR	-7.2 ± 0.2	-7.7 ± 0.2	-7.2 ± 0.1	-5.9 ± 0.2	-6.8 ± 0.2	-6.7 ± 0.2
QM PfDHFR	-7.6 ± 0.2	-7.9 ± 0.1	-7.8 ± 0.2	-6.0 ± 0.1	-7.1 ± 0.3	-7.0 ± 0.1

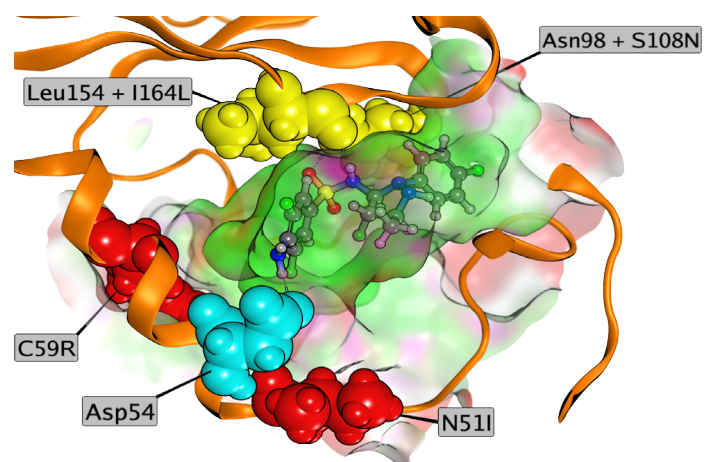


Figure 7. **7** in active site with select active site residues that contributed to binding labeled. Mutations were also labeled. Red signifies a mutated residue that did not contribute to binding. Teal signifies a non-mutated residue that contributed to binding. Yellow signifies a residue that is both mutated and contributed to binding.

a hydrogen bonding interaction contributing about -1.4 kcal/mol to the interaction energy, and -2.3 kcal/mol in hydrogen bonding interactions with Asn98. This is a direct reason why the binding energy with the quadruple mutant isoform was improved with **7**.

This result is promising because of the potential for **7** to take advantage of hydrogen bond interactions with mutated DHFR isoforms. The DHFR mutations do not seem to negatively impact interactions with **7** compared to the wild type enzymes. This is because of the right mix of lipophilicity, hydrogen bond donor/acceptors, and polarities present in the sulfonamides modeled here (Figure 7).

Ghorab and collaborators have also used this ligand framework in interactions with mitogen-activated protein kinase 2 (MAPKAPK-2), a receptor that promotes signal transduction and cell proliferations.²⁵ The ability to create multiple hydrogen bonding contacts between ligands and receptor residues drives the strong affinities observed. The impact of fluorine substituents on sulfonamide compounds has also been explored by Berrino et al., who show that varying the number and location of this polar element significantly improves binding.²⁶ The approach of fluorinating antimalarial ligands has also been detailed in an expert opinion by Upadhyay et al.²⁷ They observed that compounds with trifluoromethyl (CF₃) substituents (e.g. fluorinated triazole benzenesulfonamides) performed better than unsubstituted compounds and sulfadoxine, in complexes docked with dihydropteroate synthase, another receptor in the *P. falciparum* folate pathway. Upadhyay et al. also suggest that fluorination increases the compound's half-life, extent of absorption, metabolic stability, protein-ligand binding interactions, and excretion properties. Unlike sulfadoxine, **5-7** are also fluorinated, thus increasing their polarity and hence binding affinity. The impact of fluorination in the ligands modeled here (Figure 2, Figure 3) is consistent with literature and comparable to chlorine-based ligands like chloroquine and pyrimethamine. The rigidification of the fluorinated sulfonamides with heteroaromatic amines also enhanced the binding affinity compared to sulfadoxine (Figure 3 and 9).

The DHFR enzyme mutants modeled in this study, are causing active resistance against sulfadoxine and pyrimethamine. According to Lynch et al., I164L has been correlated with high sulfadoxine-pyrimethamine (SP) drug resistance, the mainstay drug combination in pregnant women and children 5 and below. This is because other antimalarial combinations, though effective, are more toxic to this demographic. This makes it crucial to find drugs that are able to overcome these mutations. The other mutations studied here including N51I, C59R, and S108N have also been found to create SP resistance. This SP resistance is something that was noticed in the docking studies conducted herein. When docked to the active site of DHFR, which is near the mutations, sulfadoxine and pyrimethamine had the lowest binding energies out of the ligands in this study. Whereas, the fact that **7** has interactions with I164L (Figure 7) may signify that the fluorinated-sulfonamide pharmacophore structure can help blunt the impact of some of these mutations in the development of new antimalarials.²⁸

The potential of a new and effective drug against *P. falciparum* is important, especially at a time when current antimalarials are facing decreased efficacy. For example, fluorinated sul-

fonamide-based drugs such as those studied and currently being developed could replace sulfadoxine in an artemisinin-based combined therapy (ACT).^{25,27-29} These ACTs are one of the most widely used frontline treatments of malaria. However, they are at risk of failing if artemisinin's partner drug (e.g., sulfadoxine and pyrimethamine) faces significant resistance. Development of other partner drugs could help enhance the efficacy of ACTs by mitigating the effects of resistance. This is crucial because every new drug that is developed lessens the risk of running out of effective antimalarial treatments. In addition, overdependence on current effective drugs, like artesunate, increases the risk that an impactful mutation will develop.²⁹

Conclusions

The molecular docking simulations discussed in this work identified fluorinated sulfonamide ligands as promising molecules that can be used to target critical enzymes like DHFR in the *Plasmodium* folate pathway. The estimated binding affinity of fluorinated sulfonamides docked with human and *P. falciparum* DHFR isoforms was comparable to the benchmark antimalarial drugs like artesunate, and stronger than sulfadoxine and pyrimethamine. The novel fluorinated sulfonamides (**5-7**) matched the binding affinity of artesunate to within 0.25 kcal/mol. **5-7**, also improved in binding energy from wild-type to quadruple-mutant isoforms compared to sulfadoxine. The fluorinated sulfonamide framework for drug design modeled in this study has a potential to mitigate the impacts caused by DHFR mutations. This ability to overcome mutations could lead to increased efficacy of these fluorinated sulfonamide drugs. The fluorinated sulfonamides modeled also have good drug-like characteristics based on the Lipinski rule of 5. Therefore, the novel fluorinated sulfonamides modeled can become important pharmacophores for the development of potent antimalarial drugs.

References

1. World Health Organization Malaria. <https://www.who.int/news-room/fact-sheets/detail/malaria>
2. Metz, J., Folic Acid Metabolism and Malaria. *Food and Nutrition Bulletin* **2007**, 28 (4_suppl4), S540-S549.10.1177/15648265070284s407
3. Sirawaraporn, W.; Sathitkul, T.; Sirawaraporn, R.; Yuthavong, Y.; Santi, D. V., Antifolate-resistant mutants of Plasmodium falciparum dihydrofolate reductase. *Proc Natl Acad Sci U S A* **1997**, 94 (4), 1124-9.10.1073/pnas.94.4.1124
4. Vanichtanankul, J.; Taweechai, S.; Yuvaniyama, J.; Vilaivan, T.; Chitnumsub, P.; Kamchonwongpaisan, S.; Yuthavong, Y., Trypanosomal dihydrofolate reductase reveals natural antifolate resistance. *ACS Chem Biol* **2011**, 6 (9), 905-11.10.1021/cb200124r
5. Yuthavong, Y.; Tarnchompoo, B.; Vilaivan, T.; Chitnumsub, P.; Kamchonwongpaisan, S.; Charman, S. A.; McLennan, D. N.; White, K. L.; Vivas, L.; Bongard, E.; Thongphanchang, C.; Taweechai, S.; Vanichtanankul, J.; Rattanajak, R.; Arwon, U.; Fantauzzi, P.; Yuvaniyama, J.; Charman, W. N.; Matthews, D., Malarial dihydrofolate reductase as a paradigm for drug development against a resistance-compromised target. *Proc Natl Acad Sci U S A* **2012**, 109 (42), 16823-8.10.1073/pnas.1204556109
6. Sirawaraporn, W.; Sathitkul, T.; Sirawaraporn, R.; Yuthavong,

- Y.; Santi, D. V., Antifolate-resistant mutants of *Plasmodium falciparum* dihydrofolate reductase. *Proceedings of the National Academy of Sciences* **1997**, *94* (4), 1124.10.1073/pnas.94.4.1124
7. Vanichthanukul, J.; Taweechai, S.; Uttamapinant, C.; Chitnumsub, P.; Vilaivan, T.; Yuthavong, Y.; Kamchonwongpaisan, S., Combined spatial limitation around residues 16 and 108 of *Plasmodium falciparum* dihydrofolate reductase explains resistance to cycloguanil. *Antimicrobial agents and chemotherapy* **2012**, *56* (7), 3928-3935.10.1128/AAC.00301-12
 8. Dennington, R.; Keith, T.; Millam, J., GaussView Version 5. **2009**,
 9. Frisch, M. J.; Trucks, G. W.; Schlegel, H. B.; Scuseria, G. E.; Robb, M. A.; Cheeseman, J. R.; Scalmani, G.; Barone, V.; Petersson, G. A.; Nakatsuji, H.; Li, X.; Caricato, M.; Marenich, A. V.; Bloino, J.; Janesko, B. G.; Gomperts, R.; Mennucci, B.; Hratchian, H. P.; Ortiz, J. V.; Izmaylov, A. F.; Sonnenberg, J. L.; Williams; Ding, F.; Lipparini, F.; Egidi, F.; Goings, J.; Peng, B.; Petrone, A.; Henderson, T.; Ranasinghe, D.; Zakrzewski, V. G.; Gao, J.; Rega, N.; Zheng, G.; Liang, W.; Hada, M.; Ehara, M.; Toyota, K.; Fukuda, R.; Hasegawa, J.; Ishida, M.; Nakajima, T.; Honda, Y.; Kitao, O.; Nakai, H.; Vreven, T.; Throssell, K.; Montgomery Jr., J. A.; Peralta, J. E.; Ogliaro, F.; Bearpark, M. J.; Heyd, J. J.; Brothers, E. N.; Kudin, K. N.; Staroverov, V. N.; Keith, T. A.; Kobayashi, R.; Normand, J.; Raghavachari, K.; Rendell, A. P.; Burant, J. C.; Iyengar, S. S.; Tomasi, J.; Cossi, M.; Millam, J. M.; Klene, M.; Adamo, C.; Cammi, R.; Ochterski, J. W.; Martin, R. L.; Morokuma, K.; Farkas, O.; Foresman, J. B.; Fox, D. J. *Gaussian 16 Rev. C.01*, Wallingford, CT, 2016
 10. Wishart, D. S.; Feunang, Y. D.; Guo, A. C.; Lo, E. J.; Marcu, A.; Grant, J. R.; Sajed, T.; Johnson, D.; Li, C.; Sayeeda, Z.; Assempour, N.; Iynkkaran, I.; Liu, Y.; Maciejewski, A.; Gale, N.; Wilson, A.; Chin, L.; Cummings, R.; Le, D.; Pon, A.; Knox, C.; Wilson, M., DrugBank 5.0: a major update to the DrugBank database for 2018. *Nucleic Acids Res* **2018**, *46* (D1), D1074-d1082.10.1093/nar/gkx1037
 11. Cody, V.; Pace, J.; Lin, L.; Gangjee, A., The Z isomer of 2,4-diaminofuro[2,3-d]pyrimidine antifolate promotes unusual crystal packing in a human dihydrofolate reductase ternary complex. *Acta Crystallogr Sect F Struct Biol Cryst Commun* **2009**, *65* (Pt 8), 762-766.10.1107/S1744309109025548
 12. Yuthavong, Y.; Tarnchompoo, B.; Vilaivan, T.; Chitnumsub, P.; Kamchonwongpaisan, S.; Charman, S. A.; McLennan, D. N.; White, K. L.; Vivas, L.; Bongard, E.; Thongphanchang, C.; Taweechai, S.; Vanichthanukul, J.; Rattanajak, R.; Arwon, U.; Fantauzzi, P.; Yuvaniyama, J.; Charman, W. N.; Matthews, D., Malarial dihydrofolate reductase as a paradigm for drug development against a resistance-compromised target. *Proc Natl Acad Sci U S A* **2012**, *109* (42), 16823-16828.10.1073/pnas.1204556109
 13. Berman, H. M.; Westbrook, J.; Feng, Z.; Gilliland, G.; Bhat, T. N.; Weissig, H.; Shindyalov, I. N.; Bourne, P. E., The Protein Data Bank. *Nucleic Acids Res* **2000**, *28* (1), 235-42.10.1093/nar/28.1.235
 14. Walters, W. P.; Murcko, M. A., Prediction of 'drug-likeness'. *Advanced Drug Delivery Reviews* **2002**, *54* (3), 255-271. [https://doi.org/10.1016/S0169-409X\(02\)00003-0](https://doi.org/10.1016/S0169-409X(02)00003-0)
 15. Molecular Operating Environment (MOE) *Chemical Computing Group ULC*, 2022
 16. Trott, O.; Olson, A. J., AutoDock Vina: improving the speed and accuracy of docking with a new scoring function, efficient optimization, and multithreading. *Journal of computational chemistry* **2010**, *31* (2), 455-461.10.1002/jcc.21334
 17. Pettersen, E. F.; Goddard, T. D.; Huang, C. C.; Couch, G. S.; Greenblatt, D. M.; Meng, E. C.; Ferrin, T. E., UCSF Chimera--a visualization system for exploratory research and analysis. *J Comput Chem* **2004**, *25* (13), 1605-12.10.1002/jcc.20084
 18. Ghanem, K. G.; Ram, S.; Rice, P. A., The Modern Epidemic of Syphilis. *N Engl J Med* **2020**, *382* (9), 845-854.10.1056/NEJMra1901593
 19. Al-Karmalawy, A. A.; Khattab, M., Molecular modelling of mebendazole polymorphs as a potential colchicine binding site inhibitor. *New Journal of Chemistry* **2020**, *44* (33), 13990-13996.10.1039/D0NJ02844D
 20. Vistoli, G.; Pedretti, A., 5.24 - Molecular Fields to Assess Recognition Forces and Property Spaces. In *Comprehensive Medicinal Chemistry II*, Taylor, J. B.; Triggle, D. J., Eds. Elsevier: Oxford, 2007; pp 577-602. <https://doi.org/10.1016/B0-08-045044-X/00142-5>
 21. Salas, P. F.; Herrmann, C.; Cawthray, J. F.; Nimphius, C.; Kenkel, A.; Chen, J.; de Kock, C.; Smith, P. J.; Patrick, B. O.; Adam, M. J.; Orvig, C., Structural Characteristics of Chloroquine-Bridged Ferrocenophane Analogues of Ferroquine May Obviate Malaria Drug-Resistance Mechanisms. *Journal of Medicinal Chemistry* **2013**, *56* (4), 1596-1613.10.1021/jm301422h
 22. Delaney, J. S., ESOL: Estimating Aqueous Solubility Directly from Molecular Structure. *Journal of Chemical Information and Computer Sciences* **2004**, *44* (3), 1000-1005.10.1021/ci034243x
 23. Charman, S. A.; Andreu, A.; Barker, H.; Blundell, S.; Campbell, A.; Campbell, M.; Chen, G.; Chiu, F. C. K.; Crighton, E.; Katneni, K.; Morizzi, J.; Patil, R.; Pham, T.; Ryan, E.; Saunders, J.; Shackelford, D. M.; White, K. L.; Almond, L.; Dickins, M.; Smith, D. A.; Moehrle, J. J.; Burrows, J. N.; Abba, N., An in vitro toolbox to accelerate anti-malarial drug discovery and development. *Malar J* **2020**, *19* (1), 1.10.1186/s12936-019-3075-5
 24. Soga, S.; Shirai, H.; Kobori, M.; Hirayama, N., Use of amino acid composition to predict ligand-binding sites. *J Chem Inf Model* **2007**, *47* (2), 400-6.10.1021/ci6002202
 25. Ghorab, M. M.; Alsaied, M. S.; El-Gaby, M. S. A.; Elaasser, M. M.; Nissan, Y. M., Antimicrobial and anticancer activity of some novel fluorinated thiourea derivatives carrying sulfonamide moieties: synthesis, biological evaluation and molecular docking. *Chemistry Central Journal* **2017**, *11* (1), 32.10.1186/s13065-017-0258-4
 26. Berrino, E.; Michelet, B.; Martin-Mingot, A.; Carta, F.; Supuran, C. T.; Thibaudeau, S., Modulating the Efficacy of Carbonic Anhydrase Inhibitors through Fluorine Substitution. *Angew Chem Int Ed Engl* **2021**, *60* (43), 23068-23082.10.1002/anie.202103211
 27. Upadhyay, C.; Chaudhary, M.; De Oliveira, R. N.; Borbas, A.; Kempaiah, P.; Singh, P.; Rathi, B., Fluorinated scaffolds for antimalarial drug discovery. *Expert Opin Drug Discov* **2020**, *15* (6), 705-718.10.1080/17460441.2020.1740203
 28. Lynch, C. A.; Pearce, R.; Pota, H.; Egwang, C.; Egwang, T.; Bhasin, A.; Cox, J.; Abeku, T. A.; Roper, C., Travel and the emergence of high-level drug resistance in *Plasmodium falciparum*

- parum in southwest Uganda: results from a population-based study. *Malar J* **2017**, *16* (1), 150.10.1186/s12936-017-1812-1
29. Mita, T.; Tanabe, K., Evolution of Plasmodium falciparum drug resistance: implications for the development and containment of artemisinin resistance. *Jpn J Infect Dis* **2012**, *65* (6), 465-75.10.7883/yoken.65.465